Available online at www.sciencedirect.com
ScienceDirect
Journal of Sound and Vibration 304 (2007) 391–399
JOURNAL OF SOUND AND VIBRATION
www.elsevier.com/locate/jsvi

Short Communication

A note on the dynamics of a vibromachine with parametric excitation

Wang Lin*, Ni Qiao

Department of Mechanics, Huazhong University of Science & Technology, Wuhan 430074, PR China

Received 17 November 2006; received in revised form 13 February 2007; accepted 16 February 2007

Abstract

In this note, the dynamics of a vibration machine with piecewise linear elastic ties under parametric harmonic excitation is further investigated. Attention was concentrated on the dynamical behaviour of the system in the regions of several system parameters, both with and without physically realistic parameters. Based on numerical simulations, several typical motions were found, showing some new and interesting results. Chaos, as well as periodic motion was found readily for physically unrealistic parameters. The route to chaos is shown to be via period-doubling bifurcations. For the physically realistic parameters, however, chaotic motion with small amplitude oscillations was found.

1. Introduction

As it may be of significant importance in the design of structural machine members and control of engineering vibromachines, the dynamics of various mechanical elements with periodically time-varying elasticity has been investigated in the past decades [1–5]. Recently, Belovodsdy et al. [6] revealed the parametric oscillations of a technological vibromachine which may be widely used in the form of a rotating disk (Fig. 1). In the study of Ref. [6], some peculiarities of nonlinear parametric oscillations are shown and the bounds of the region of parametric instability obtained by analysing solutions of the equations of motion for the vibromachine system.

It is noted that, in Ref. [6], no bifurcation diagrams were presented, and no chaos was found. Hence, the possible complex behaviours, including various periodic and non-periodic motions, have not been shown in detail yet. To address the lack of research in this respect, the present study analyses numerically the possible chaotic behaviours in such a vibromachine system developed in Ref. [6] with the emphasis on the detailed dynamics via several bifurcation diagrams as the system parameters are varied.

2. Background theory

As shown in Fig. 1, the disk consists of two rings, 1 and 2, connected one with another by elastic elements (springs 3). Internal ring 1 is slipped over on a rigid solid shaft 4, but external ring 2, through balls 5, is

*Corresponding author. Tel.: +86 27 87543438.
E-mail address: wanglinfliping@sohu.com (W. Lin).

0022-460X/$ - see front matter
doi:10.1016/j.jsv.2007.02.018

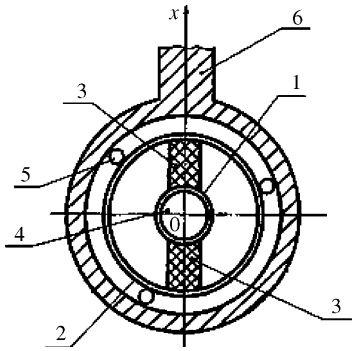

Fig. 1. Schematic of the parametric elastic element in the form of a rotating disk: 1 and 2, internal and external rigid rings; 3, elastic elements (springs); 4, rigid solid shaft; 5, bearings; 6, working head of vibromachine.

connected with the working head 6 of the vibromachine. Moreover, upon rotation of shaft 4 the elasticity of the disk in the radial direction is periodically changed. Thus, parametric vibrations of working head 6 are excited. In practice, parametric excitation may be realized by pneumatic elastic elements with variable air pressure.

To analyse the above vibromachine model, the authors of Ref. [6] have developed it to be a single-degree-of-freedom vibratory system (Fig. 2). In forming a mathematical model of the vibromachine some assumptions were made: working head is considered as a perfectly rigid body; driving motor as ideal; damping in elastic supports as viscous and its is also assumed that the elastic supports 3 are not deformed when the machine is in static equilibrium.

Under these assumptions, the differential equation of vibrations of the working head of the vibromachine can be represented as [6]

$$m\frac{\mathrm{d}^2x}{\mathrm{d}t^2}+b(x)\frac{\mathrm{d}x}{\mathrm{d}t}+b(1+\mu_1\sin\,\Omega t)\frac{\mathrm{d}x}{\mathrm{d}t}+F_r(x)+k_0(1+\mu_1\sin\,\Omega t)x=0, \tag{1}$$

in which x is the coordinate of the working head, t the time, m the mass of the working head, $b(x)$ the nonlinear function describing damping in the main and additional elastic supports, b the damping coefficient of the parametric elastic element, $F_r(x)$ the nonlinear function describing the elastic characteristic of the supports, k_0 the average stiffness coefficient of the parametric elastic element, μ_1 the dimensionless amplitude of the parametric excitation, Ω the frequency of the parametric excitation.

Moreover, functions $b(x)$ and $F_r(x)$ in Eq. (1) can be expressed as

$$b(x)=\left\{\begin{array}{ll} b_1(k_1+k_2)/k_1, & x\geqslant\Delta^+ \\ b_1, & k-\Delta^-<x<\Delta^+ \\ b_1(k_1+k_2)/k_1, & x\leqslant-\Delta^- \end{array}\right\}, \tag{2}$$

$$F_r(x)=\left\{\begin{array}{ll} (k_1+k_2)x-k_2\Delta^+, & x\geqslant\Delta^+ \\ k_1x, & -\Delta^-<x<\Delta^+ \\ (k_1+k_2)x+k_2\Delta^-, & x\leqslant-\Delta^- \end{array}\right\}, \tag{3}$$

in which k_1 is the stiffness coefficient of the main elastic supports, k_2 is the stiffness coefficient of the elastic limiters, Δ^+ and Δ^- are the initial clearances between the working head and the elastic limiters.

Introducing the following notation:

$$y=\frac{x}{\Delta^-},\ \ \tau=\omega_0t=\sqrt{\frac{k_1+k_2}{m}}t,\ \ \eta=\frac{\Omega}{\omega_0},\ \ \mu=\mu_1\frac{k_0}{k_1+k_2},\ \ k=\frac{k_1+k_2+k_0}{k_1+k_0},$$
$$\beta=\frac{b}{\sqrt{(k_1+k_0)m}},\ \ \beta_1=\frac{b_1}{\sqrt{(k_1+k_0)m}},\ \ \Delta^*=\frac{\Delta^+}{\Delta^-}, \tag{4}$$

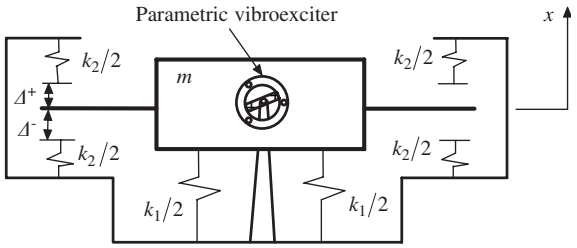

Fig. 2. Vibromachine model considered in the analysis.

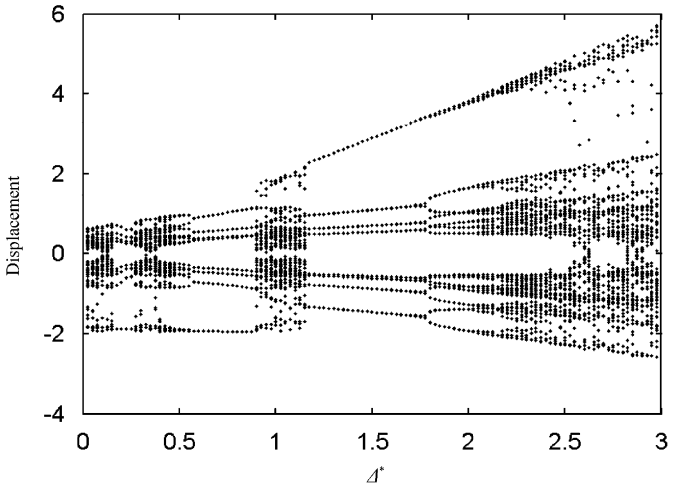

Fig. 3. Bifurcation diagram of the vibration for $\beta = 0.05$, $\eta = 0.25$, $\mu = 1.5$, $\beta_1 = 0.05$, $k = 3$ and $\beta^* = 0.051$, as Δ^* is varied.

Eq. (1) and functions (2) and (3) can be transformed into the dimensionless forms

$$\frac{d^2y}{d\tau^2} + \beta(y)\frac{dy}{d\tau} + \beta(1 + \mu \sin \eta\tau)\frac{dy}{d\tau} + f_r(y) + (\mu \sin \eta\tau)y = 0, \tag{5}$$

$$\beta(y) = \left\{ \begin{array}{ll} \beta_1(k_1 + k_2)/k_1, & y \geqslant \Delta^* \\ \beta_1, & -1 < y < \Delta^* \\ \beta_1(k_1 + k_2)/k_1, & y \leqslant -1 \end{array} \right\}, \tag{6}$$

$$f_r(y) = \left\{ \begin{array}{ll} ky - (k-1)\Delta^*, & y \geqslant \Delta^* \\ y, & -1 < y < \Delta^* \\ ky + (k-1), & y \leqslant -1 \end{array} \right\}. \tag{7}$$

Thus, by analysing solutions of Eqs. (5)–(7), the nonlinear dynamics of the vibromachine system can be revealed. However, other than Ref. [6], most attention of this work is concentrated on the possible chaotic motions in several parameter regions of the dynamical system, as represented below.

3. Bifurcation diagrams and typical behaviours of the system

As mentioned in the foregoing, for such a vibration system considered in this short communication, its parametric oscillations have been investigated in Ref. [6]. Moreover, this system is fast becoming an important model in dynamics. However, as there are many system parameters in this model, it is capable of displaying

much richer dynamical behaviour, for instance, nonlinear and chaotic dynamics. The more important of them are considered in what follows.

Solutions of Eq. (5) were obtained by using a fourth-order Runge–Kutta integration algorithm, where a novel approach for solving dynamical systems with motion dependent discontinuities [7] was also utilized. The initial conditions employed were $y(0) = 0.02,\ \dot{y}(0) = 0$.

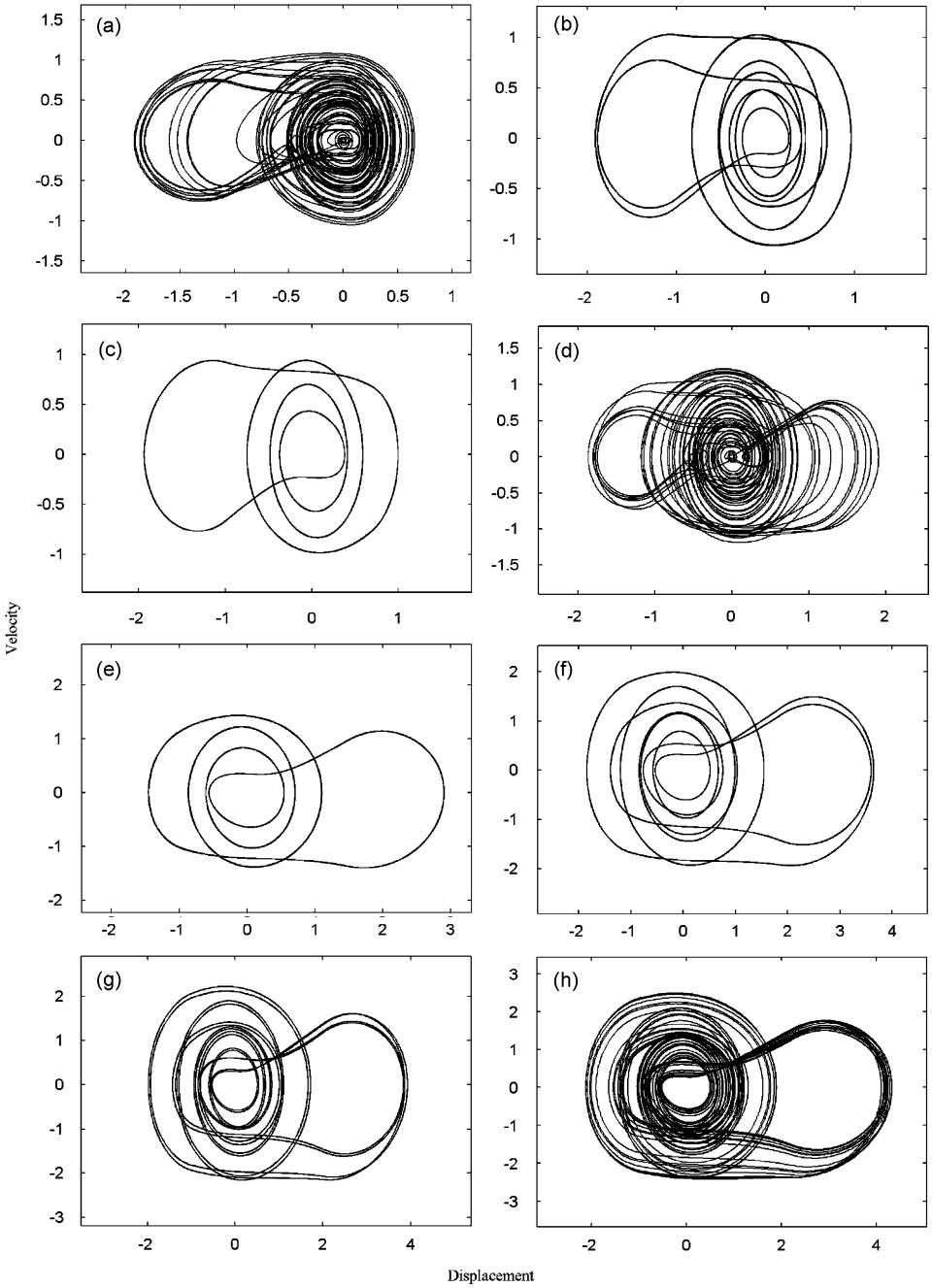

Fig. 4. Phase-plane plots for the system of Fig. 3, and various values of Δ^*: (a) $\Delta^* = 0.05$; (b) $\Delta^* = 0.5$; (c) $\Delta^* = 0.7$; (d) $\Delta^* = 1.0$; (e) $\Delta^* = 1.5$; (f) $\Delta^* = 1.9$; (g) $\Delta^* = 2.05$; (h) $\Delta^* = 2.25$.

The bifurcation diagram can provide a summary of essential dynamics and is therefore a useful tool for acquiring this overview. Fig. 3 shows the bifurcation diagram of the displacement as Δ^* is varied. In this figure the displacement plotted in the ordinate is the amplitude of the vibration. In the calculations, the transient solutions were discarded. Then, whenever the velocity of the vibration was zero (i.e., $\dot{y}(\tau) = 0$), the displacement ($y(\tau)$) was recorded. Fig. 3 indicates that, with the increase of Δ^*, complex bifurcation routes can be detected. When Δ^* is very small (e.g, $\Delta^* = 0.05$), the dynamical system may undergo a chaotic motion. Moreover, in the range $0 < \Delta^* < 1.175$, there are relatively large regions of periodic motions embedded within the chaotic region; e.g., for $0.6 < \Delta^* < 0.85$ there is what appears to be a period-8 region. At about $\Delta^* = 1.2$, a period-8 motion occurs again. Then this period-8 motion evolves to a period-16 one at $\Delta^* \approx 1.775$. Clearly, a sequence of period-doubling bifurcations is visible as Δ^* is increased gradually. Hence, this period-doubling bifurcations lead the system to chaos, as can be seen in Fig. 3. Finally, it should be remarked that the positive displacement amplitude of the system becomes larger with increasing Δ^*.

It is instructive to look at phase-plane portraits associated with various values of Δ^*, corresponding to different dynamical behaviour as discussed in the forgoing. For this purpose, the physical displacements of the system are plotted against the corresponding velocities. Sample results are shown in Fig. 4.

Of course, similar bifurcation diagrams may be constructed with each of the system parameters as a variable. Fig. 5 shows one such diagram, with the frequency parameter, η, as the variable parameter. In this case, fixed point, chaotic and periodic motions occur as η is varied gradually. The phase-plane portraits of several typical dynamical behaviours are further represented in Fig. 6. Fig. 7 shows the bifurcation diagram as $\beta^*(\beta^* = \beta_1(k_1 + k_2)/k_1)$ is varied. When β^* is small, chaotic motion can be clearly seen. However, the system always undergoes a periodic motion with a large value of β^*. If we choose β to be the variable parameter, Fig. 8 has shown that the system always undergoes chaotic motion in the range $0 < \beta < 0.09$. Figs. 9 and 10 represent the bifurcation diagrams as β_1 and k are varied, respectively.

In all the results presented in Figs. 3–10, it ought to be noted that the value of amplitude of parametric excitation was selected to be $\mu = 1.5$. Notice, however, such great value of μ is difficult to be realized in practice with the aid of parametric elastic element shown in Fig. 1. Coefficient μ is always under 1 ($\mu < 1$) for this parametric element. Thus, more extensive calculations have been carried out for physically realistic parameters: $\beta^* = 3$, $\Delta^* = 1$, $k = 3$, $\beta_1 = 0.005$, $\beta = 0.005$ and $\mu = 0.8$. In this case, the frequency of the parametric excitation η is varied. The principally findings of numerical calculations were two. First, for these physically realistic parameters, the system can also display periodic motions. Sample results are shown in Fig. 11. Second, it is interesting to note that for many parameter ranges of η, the amplitude of the oscillation is very small. Typical diagrams of phase portrait and power spectrum of the vibrations are shown in Fig. 12. Indeed, in this figure, the small-amplitude vibrations are demonstrated to be chaotic, as can be clearly seen. However, no chaotic motions with large amplitude oscillations have been detected. Hence, with increasing η, the

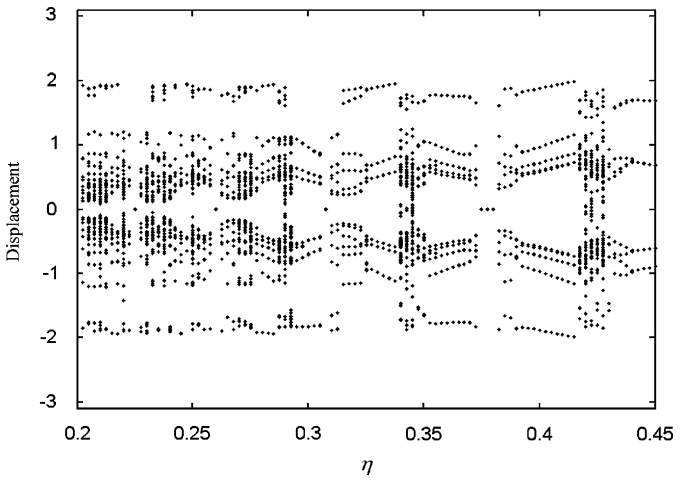

Fig. 5. Bifurcation diagram of the vibration for $\beta = 0.05$, $\Delta^* = 1$, $\mu = 1.5$, $\beta_1 = 0.05$, $k = 3$ and $\beta^* = 0.051$, as η is varied.

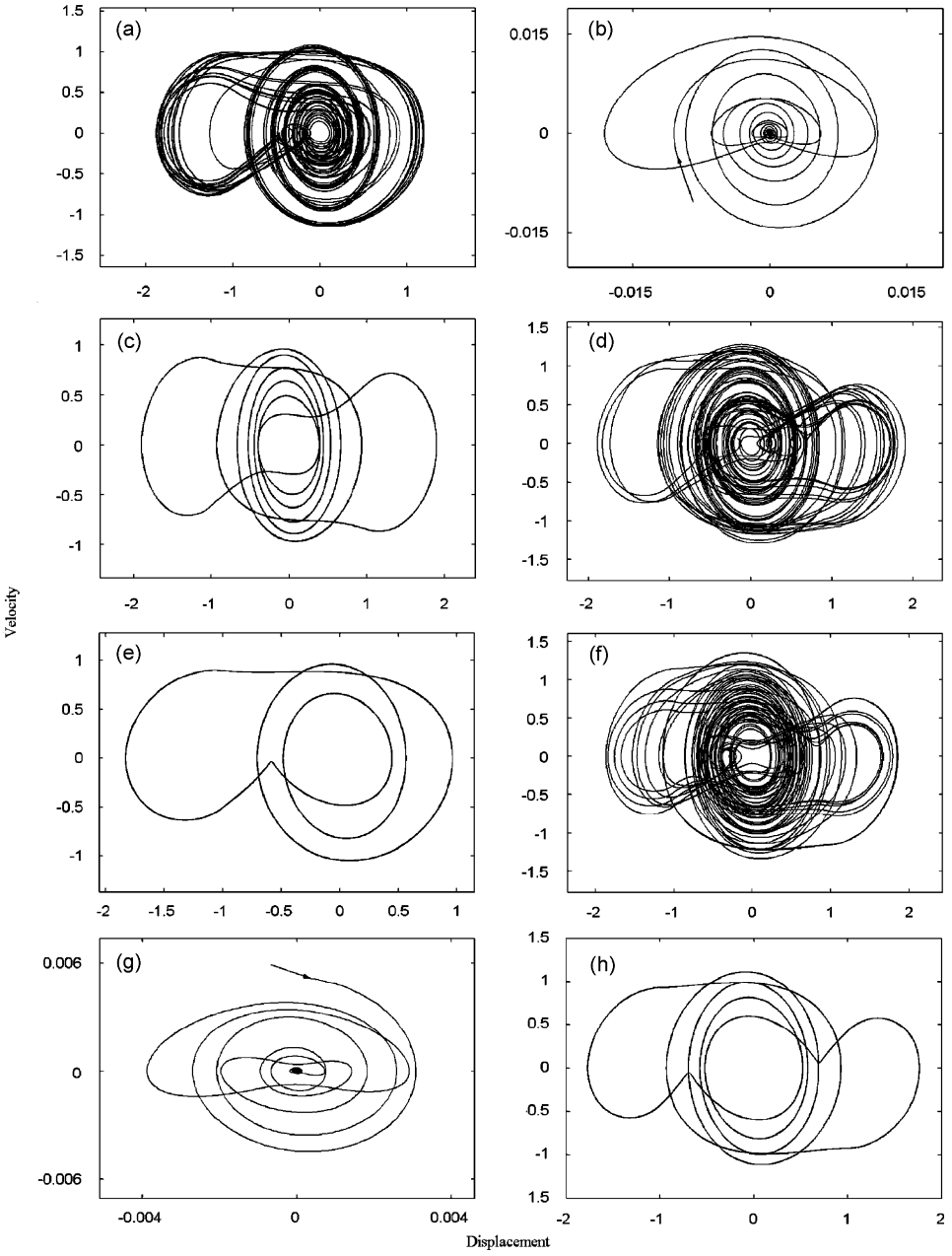

Fig. 6. Phase-plane plots for the system of Fig. 5, and various values of η: (a) $\eta = 0.22$; (b) $\eta = 0.225$; (c) $\eta = 0.275$; (d) $\eta = 0.278$; (e) $\eta = 0.29$; (f) $\eta = 0.30$; (g) $\eta = 0.345$; (h) $\eta = 0.36$.

amplitude of the vibration may jump from a large one (corresponding to a periodic motion) to a small one (corresponding to a chaotic motion), or from a small one to a large one, the nature of which is not understood.

4. Conclusion

Bifurcation and chaos of a working head of the vibromachine are numerically investigated via the calculations of bifurcation diagrams, phase portraits and power spectrum diagrams. The behaviour was analysed without physical realism to see the character of the system response, and chaos was found as well as

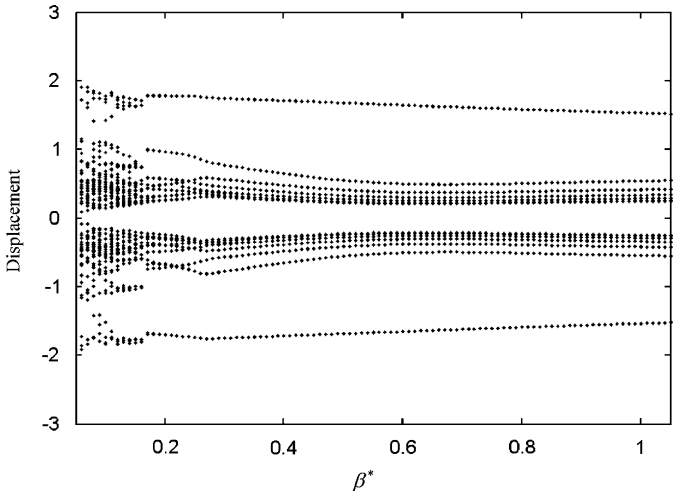

Fig. 7. Bifurcation diagram of the vibration for $\beta = 0.05$, $\Delta^* = 1$, $\mu = 1.5$, $\beta_1 = 0.05$, $k = 3$ and $\eta = 0.25$, as β^* is varied.

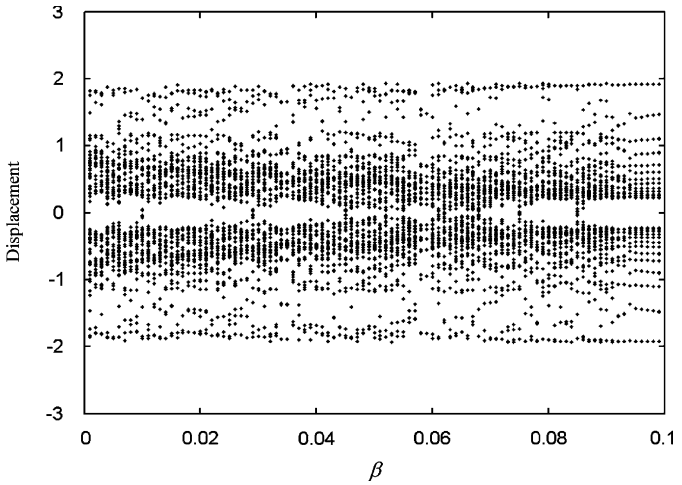

Fig. 8. Bifurcation diagram of the vibration for $\beta^* = 0.051$, $\Delta^* = 1$, $\mu = 1.5$, $\beta_1 = 0.05$, $k = 3$ and $\eta = 0.25$, as β is varied.

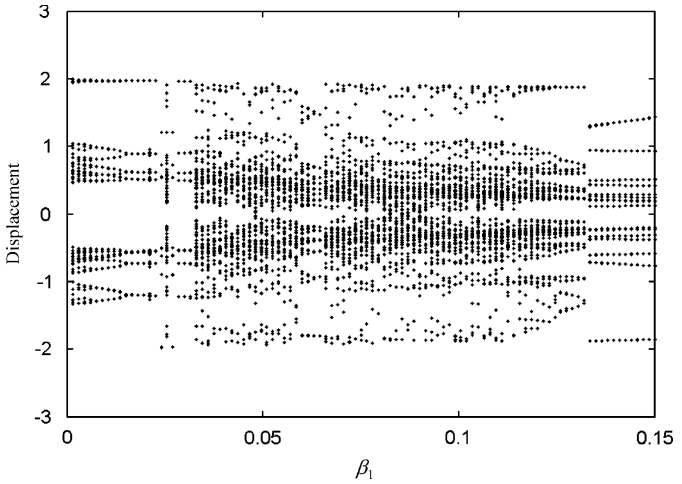

Fig. 9. Bifurcation diagram of the vibration for $\beta^* = 0.051$, $\Delta^* = 1$, $\mu = 1.5$, $\beta = 0.05$, $k = 3$ and $\eta = 0.25$, as β_1 is varied.

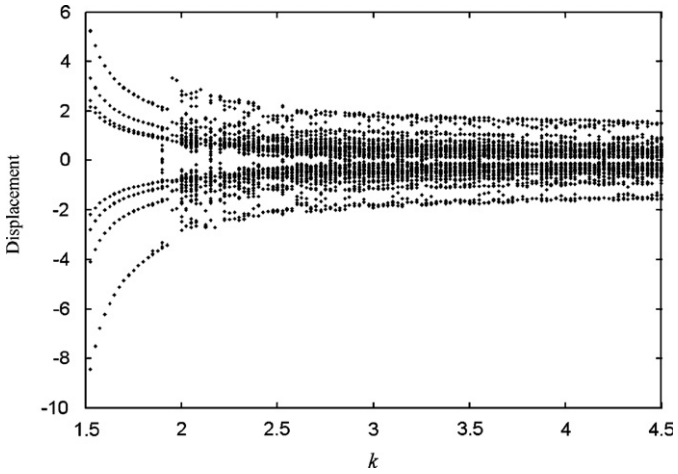

Fig. 10. Bifurcation diagram of the vibration for $\beta^* = 0.051$, $\Delta^* = 1$, $\mu = 1.5$, $\beta_1 = 0.05$, $\beta = 0.05$ and $\eta = 0.25$, as k is varied.

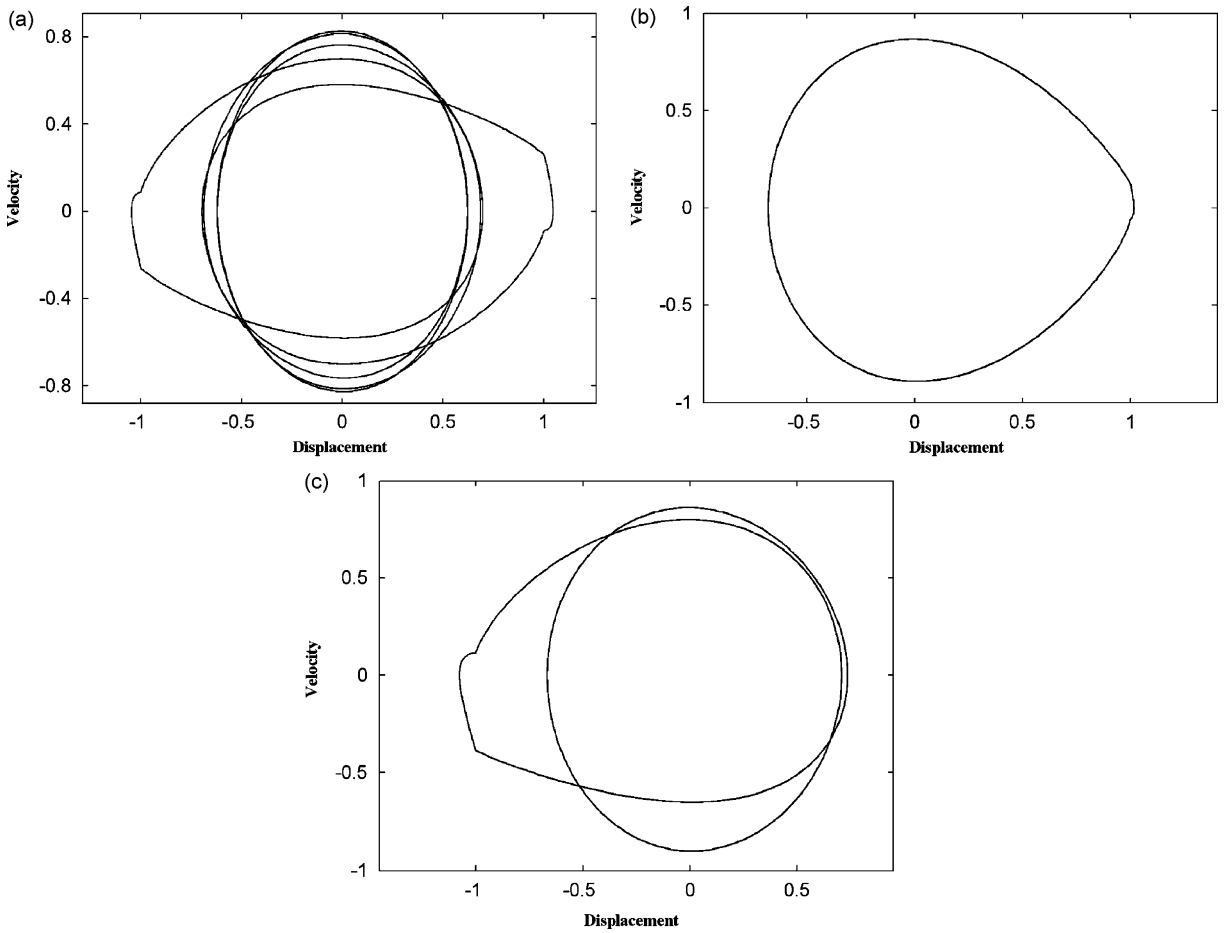

Fig. 11. Phase portraits of periodic motions for physically realistic parameters: (a) $\eta = 0.378$; (b) $\eta = 0.875$; (c) $\eta = 0.475$.

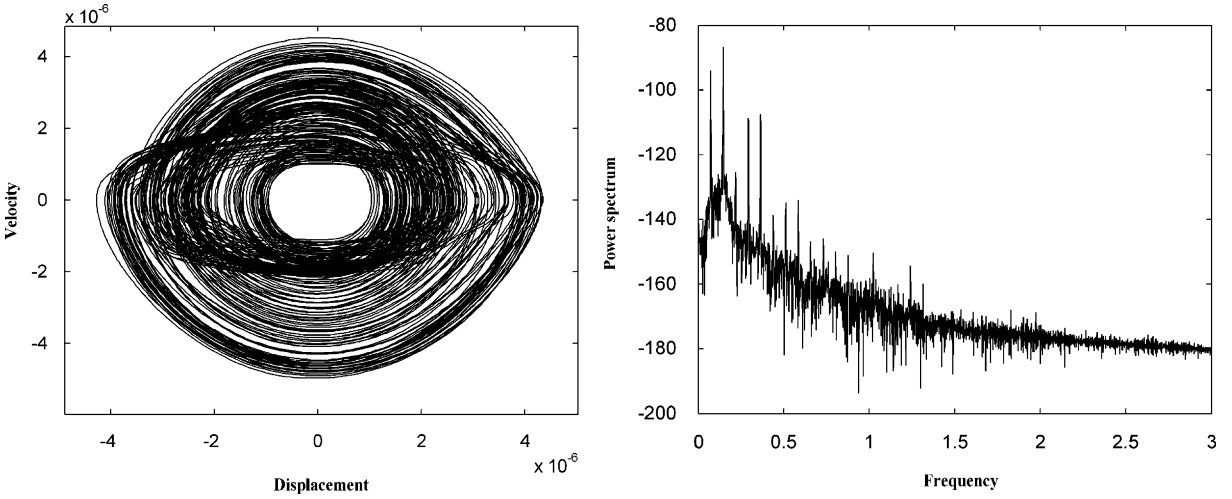

Fig. 12. Phase portrait and power spectrum of the vibration for physically realistic parameters, and $\eta = 1.378$.

periodic motions. Then the behaviour with physical meaning was analysed to see what nonlinear behaviour would be predicted for physically realistic responses, and chaotic motions with very small amplitude of oscillations were found. Hence, the dynamical behaviour of the vibromachine is extremely rich and sometimes unexpected.

The present research may be extended to deal with some nonlinear problems of vibromachines, which may be of significant importance in designing technological vibromachines with external excitation. Obviously, various periodic motions, and in particular, the chaotic responses should be determined.

Acknowledgements

The research was supported by grant from the National Nature Science Foundation of China (No. 10272051) and the Nature Science Foundation of HUST (No. 2006Q003B), to whom the authors express their deep gratitude. The comments and suggestions made by the anonymous referees are also gratefully appreciated.

References

[1] P.R. Pagilla, B. Yu, K.L. Pau, Adaptive control of time-varying mechanical systems: analysis and experiments, *IEEE/American Society of Mechanical Engineers Transactions on Mechatronics* 5 (2000) 410–418.

[2] S. Tsyfansky, V.I. Beresnevich, Mathematical simulation of dynamics of textile machines on specialized analog-digital computational complex, *Proceedings of the 5th International Conference of Cranes and Textile Machines*, Gdansk, Poland, 1996, pp. 257–260.

[3] S.L. Tsyfansky, V.I. Beresnevich, The control of the operating condition of a subharmonic vibromachine, *Journal of Sound and Vibration* 203 (1998) 495–503.

[4] M. Ruijgrok, K. Verhulst, Parametric and autoparametric resonance, *Progress in Nonlinear Differential Equations and their Applications* 19 (1996) 279–298.

[5] R. Svoboda, A. Tondl, F. Verhulst, Autoparametric resonance by coupling of linear and non-linear systems, *International Journal of Non-Linear Mechanics* 29 (1994) 225–232.

[6] V.N. Belovodsky, S.L. Tsyfansky, V.I. Beresnevich, The dynamics of a vibromachine with parametric excitation, *Journal of Sound and Vibration* 254 (2002) 897–910.

[7] M. Wiercigroch, Modelling of dynamical systems with motion dependent discontinuities, *Chaos, Solitons and Fractals* 11 (2000) 2429–2442.